Supplemental Information

Table S1 Key resources in experiments

REAGENT or RESOURCE	SOURCE	IDENTIFIER
Antibodies		
Rabbit Anti-CaMKIIa	Abcam	Cat#ab5683; RRID: AB_305050; 1:500
DyLight 647 Goat Anti-Rabbit	Thermo Fisher Scientific	Cat#a-21244; RRID: AB_2535812; 1:300
Bacterial and Virus Strains		
AAV2/9-hSyn-DIO-hM4D(Gi)-mCherry	BrainVTA, Wuhan	Cat# PT-0020
AAV2/9-hSyn-DIO-hM3D(Gq)-mCherry	BrainVTA, Wuhan	Cat# PT-0019
AAV2/1-hSyn-Cre	BrainVTA, Wuhan	Cat# PT-0136
AAV2/9-hEF1a-WGA-Cre	Taitool, Shanghai	Cat# S0860-9
AAV2/9-hSyn-DIO-mCherry	BrainVTA, Wuhan	Cat# PT-0115
AAV2/9-hSyn-DIO-EGFP	BrainVTA, Wuhan	Cat# PT-1103
AAV2/9-EF1a-DIO-GCaMP6f	Taitool, Shanghai	Cat# S0588-9
AAV2/9-EF1α-DIO-ChR2-EGFP	BrainVTA, Wuhan	Cat# PT-0002
AAV2/9-EF1α-DIO-eNpHR3-EGFP	BrainVTA, Wuhan	Cat# PT-0007
rAAV2/2-hSyn-Retro-Cre	Brain case, Shenzhen	Cat#BC-0160
AAV2/2-hSyn-Retro-FLP	BrainVTA, Wuhan	Cat#PT-0341
AAV2/2-hSyn-Retro-EGFP	BrainVTA, Wuhan	Cat#PT-1990
rAAV2/2-hSyn-Retro-Cre-EGFP	Brain case, Shenzhen	Cat#BC-0160
AAV-hSyn-Con/Fon-hM3Dq(Gq)-EGFP	BrainVTA, Wuhan	Cat#PT-2368
AAV-hSyn-Con/Fon-hM4Di(Gi)-EGFP	BrainVTA, Wuhan	Cat#PT-1572
AAV-hSyn-Con/Fon-EGFP	BrainVTA, Wuhan	Cat#PT-0169
AAV-hSyn-Con/Fon-eNpHR3-EGFP	BrainVTA, Wuhan	Cat#PT-1154
AAV-EF1a-Flex-taCasp3	BrainVTA, Wuhan	Cat#PT-0206
Chemicals, Peptides, and Recombinant Proteins		
Clozapine N-oxide (CNO)	Sigma-Aldrich	Cat# C0832
Green Retrobeads	Lumafluor	Cat# G180
4-Aminopyridine(4-AP)	Tocris	Cat# 0940
CNQX	Tocris	Cat# 0190
Tetrodotoxin (TTX)	Tocris	Cat# 1078
Bicuculine	Tocris	Cat# 14340
Software and Algorithms		
GraphPad Prism 8	GraphPad Software	N/A
ImageJ	NIH	https://imagej.nih.gov/ij
Excel	Microsoft	N/A

Photoshop CS5	Adobe	N/A
MATLAB 2014a and 2017a	MathWorks	N/A
Clampfit 10.0	Molecular Devices	N/A

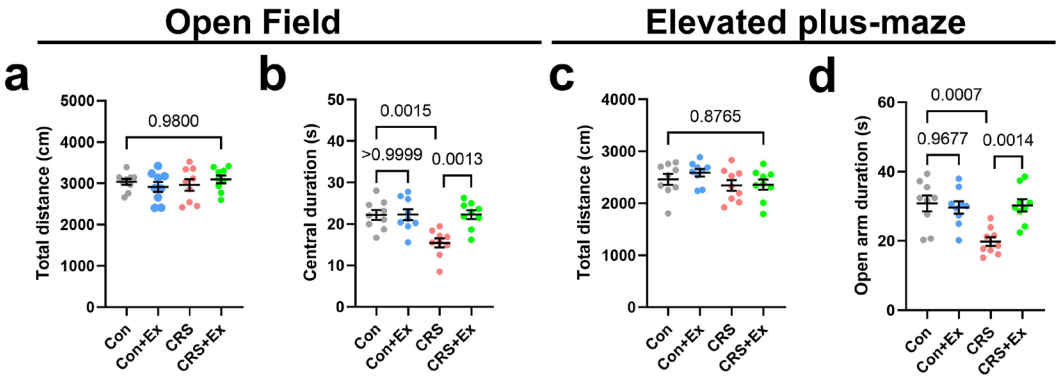

Figure S1. Treadmill exercise relives chronic restraint stress-induced anxiety-like disorders. **(a)** Exercise training did not change overall locomotor ability in the open field. $F(3,32)=0.5462$, $P=0.6543$. **(b)** Exercise increased time spent in the central region in CRS mice but not in naïve ones. $F(3,32)=8.466$, $P=0.0003$. **(c)** Treadmill exercise did not affect the total distance travelled on the elevated plus-maze. $F(3,32)=1.360$, $P=0.2725$. **(d)** Exercise training increased the time spent in the open arm region only in CRS mice. $F(3,32)=8.538$, $P=0.0003$. $N=9$ mice each group. Tukey's multiple comparison test was employed to make comparisons between two specified groups. All data were presented as mean±sem.

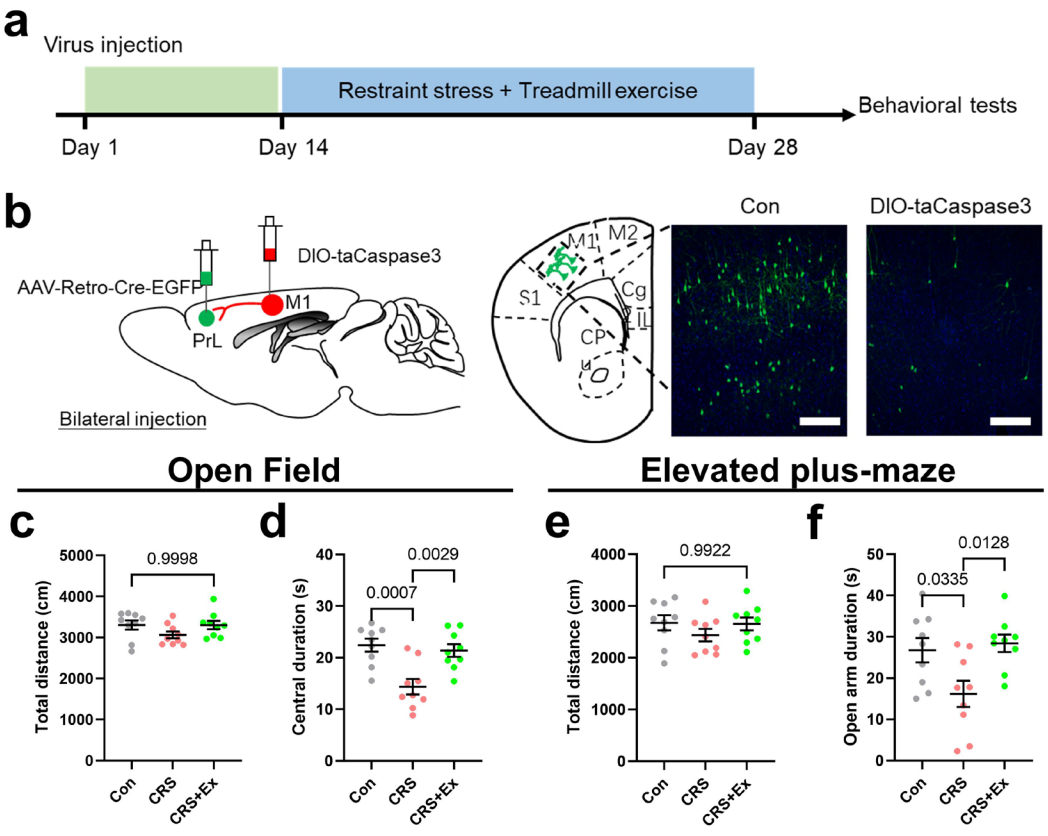

Figure S2. M1-PrL pathway is not involved in exercise-mediated anxiolysis. (a) Timelines of experimental design. **(b)** Left, viral injection sites; Right, density of PrL-projecting M1 neurons under cell ablation. Green, EGFP. Scale bar, 150 μm. **(c)** The ablation of PrL-projecting M1 neurons did not change overall locomotor ability in the open field. One-way ANOVA, $F(2,24)=1.933$, $P=0.1666$. **(d)** Specific cell ablation did not affect the exercise effect in increasing central region duration. $F(2,24)=10.84$, $P=0.0004$. **(e)** The cell ablation did not affect the total distance travelled on the elevated plus-maze. $F(2,24)=1.046$, $P=0.3668$. **(f)** The ablation of M1-PrL pathway did not affect the exercise effect in increasing the time spent in the open arm region. $F(2,24)=5.682$, $P=0.0095$. $N=9$ mice each group. Tukey's multiple comparison test was employed to make comparisons between two specified groups. All data were presented as mean±sem.

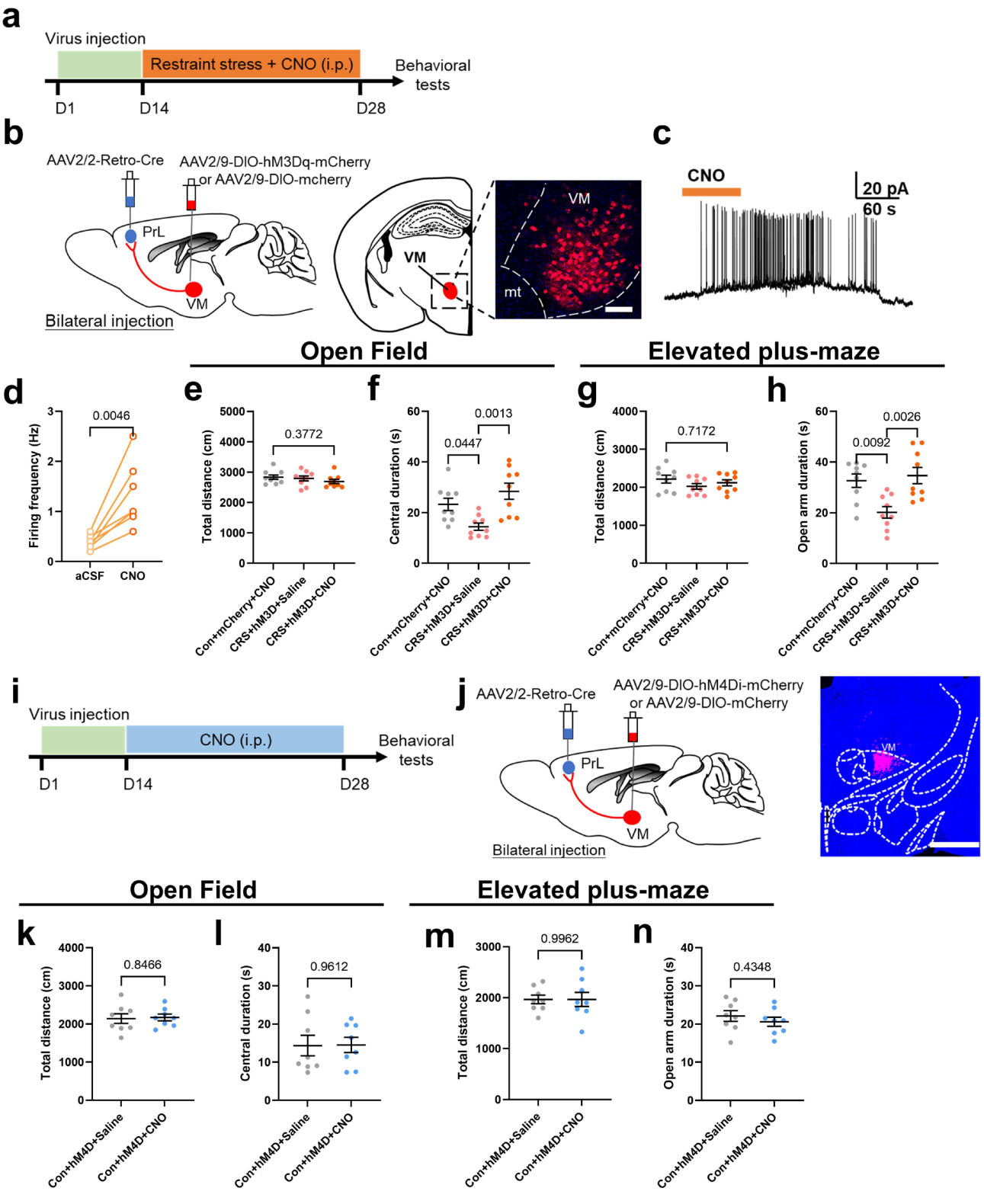

Figure S3. VM-PrL circuit unidirectionally modulates anxiety-like behaviors. (a) Timelines of experimental design for the chemogenetic activation of PrL-projecting VM neurons. **(b)** Left, viral injection sites. Right, PrL-projecting VM neurons. Red, mCherry. Scale bar, 100 μm. **(c)**

Sample traces of VM neurons giving under CNO infusion. **(d)** CNO infusion effectively increased cellular excitability. Paired *t*-test, $t(6)=4.390$, $P=0.0046$. $n=7$ neurons from 3 mice. **(e)** Chemogenetic activation (CNO group) did not change overall locomotor ability in the open field. $F(2,24)=0.9740$, $P=0.3920$. **(f)** CNO infusion increased time spent in the central region. $F(2,24)=8.359$, $P=0.0018$. **(g)** The chemogenetic manipulation did not affect the total distance travelled on the elevated plus-maze. $F(2,24)=1.214$, $P=0.3146$. **(h)** The chemogenetic activation of PrL-projecting VM neurons increased the time spent in the open arm region. $F(2,24)=8.359$, $P=0.0018$. $N=9$ mice each group in **(e-h)**. Tukey's multiple comparison test was employed to make comparisons between two specified groups. **(i)** Timelines of experimental design for the chemogenetic inhibition of PrL-projecting VM neurons. **(j)** Left, viral injection sites. Right, PrL-projecting VM neurons. Red, mCherry. Scale bar, 500 μm. **(k)** Chemogenetic inhibition (CNO group) did not change overall locomotor ability in the open field. Two-sampled unpaired *t*-test, $t(14)=0.1971$, $P=0.8466$. **(l)** CNO infusion did not change the time spent in the central region. $t(14)=0.04959$, $P=0.9612$. **(m)** The chemogenetic manipulation did not affect the total distance travelled on the elevated plus-maze. $t(14)=0.004854$, $P=0.9962$. **(n)** The chemogenetic inhibition of PrL-projecting VM neurons did not affect the time spent in the open arm region. $t(14)=0.8041$, $P=0.4348$. $N=8$ mice each group in **(k-n)**. All data were presented as mean±sem.

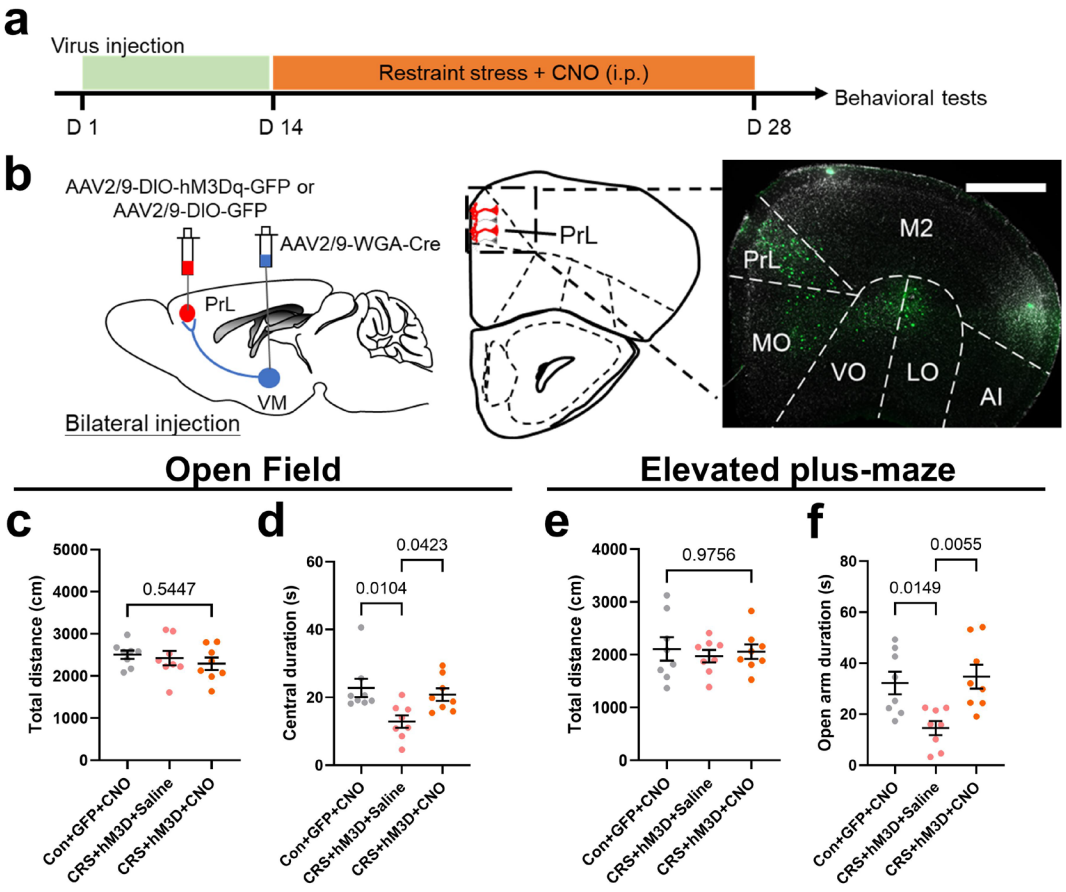

Figure S4. Chemogenetic activation of PrL neurons at the downstream of VM mimics exercise effect in anxiolysis. (a) Timelines of experimental design. **(b)** Left, viral injection schemes. Right, distribution of VM innervating neurons in PrL. Green, GFP. Scale bar, 250 μm. **(c)** Chemogenetic manipulation did not change overall locomotor ability in the open field. $F(2,21)=0.5787$, $P=0.5693$. **(d)** The activation of PrL neurons increased time spent in the central region. $F(2,21)=5.903$, $P=0.0092$. **(e)** CNO infusion did not affect the total distance travelled on the elevated plus-maze. $F(2,21)=0.1739$, $P=0.8416$. **(f)** Chemogenetic activation of VM-PrL pathway increased the time spent in the open arm region. $F(2,21)=7.363$, $P=0.0038$. $N=8$ mice each group. Tukey's post-hoc test was employed to make comparisons between two specified groups. All data were presented as mean±sem.

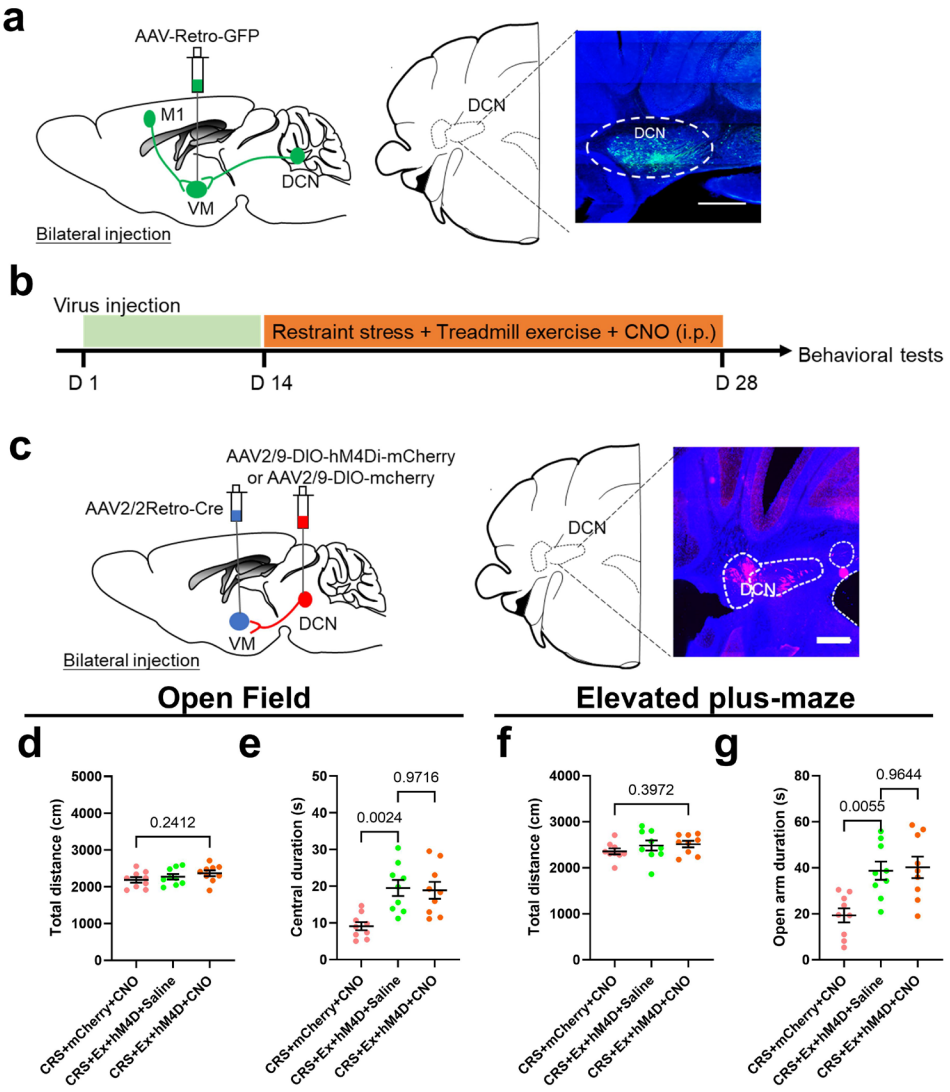

Figure S5. DCN-VM pathway did not mediate anxiolytic effect of exercise training. (a) Left, viral injection schemes. Right, distribution of VM innervating neurons in DCN. Green, GFP. Scale bar, 100 μm. **(b)** Timelines of experimental design. **(c)** Left, viral injection sites. Right, distribution of VM innervating neurons in DCN. Red, mCherry. Scale bar, 100 μm. **(d)** Chemogenetic manipulation did not change overall locomotor ability in the open field. $F(2,24)=1.382$, $P=0.2412$. **(e)** The activation of DCN neurons did not affect the time spent in the central region in exercised group. $F(2,24)=9.074$, $P=0.0012$. Tukey's post-hoc comparison, Saline vs CNO, $P=0.9716$. **(f)** CNO infusion did not affect the total distance travelled on the elevated plus-maze. $F(2,24)=0.9823$,

P=0.3972. **(g)** Chemogenetic activation of DCN-VM pathway did not affect the time spent in the open arm region under exercise intervention. $F(2,24)=8.630$, *P*=0.0015. Tukey's post-hoc comparison, Saline vs CNO, *P*=0.9644. *N*=9 mice each group. All data were presented as mean± sem.

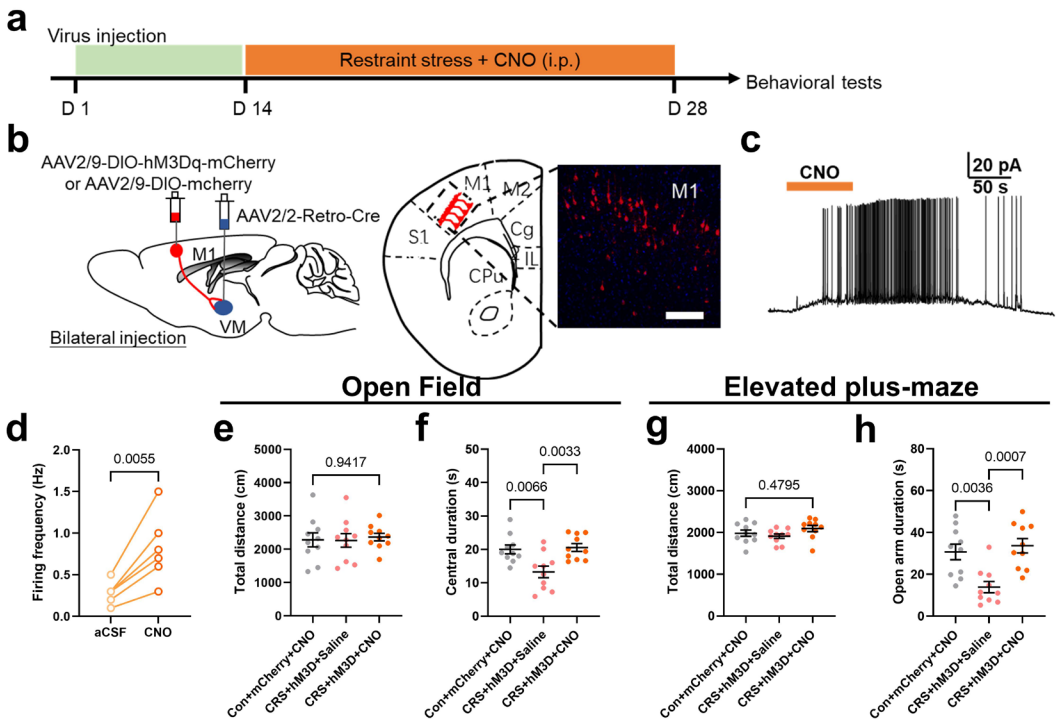

Figure S6. Chemogenetic activation of VM-projecting M1 neurons recapitulates exercise effects in relieving anxiety-like behaviors. (a) Timelines of experimental design. **(b)** Left, viral injection sites. Right, distribution of VM projecting neurons in M1. Red, mCherry. Scale bar, 100 μm. **(c)** Sampled traces of M1 neurons under CNO infusion. **(d)** CNO infusion effectively increased cellular excitability. Paired *t*-test, $t(5)=4.658$, $P=0.0055$. $n=6$ neurons from 3 mice. **(e)** Chemogenetic activation (CNO group) did not change overall locomotor ability in the open field. $F(2,27)=0.08899$, $P=0.9151$. **(f)** CNO infusion increased time spent in the central region. $F(2,27)=8.146$, $P=0.0017$. **(g)** The chemogenetic manipulation did not affect the total distance travelled on the elevated plus-maze. $F(2,27)=1.850$, $P=0.1766$. **(h)** The chemogenetic activation of VM-projecting M1 neurons increased the time spent in the open arm region. $F(2,27)=10.40$, $P=0.0004$. $N=10$ mice each group. Tukey's multiple comparison test was employed to make comparisons between two specified groups. All data were presented as mean±sem.

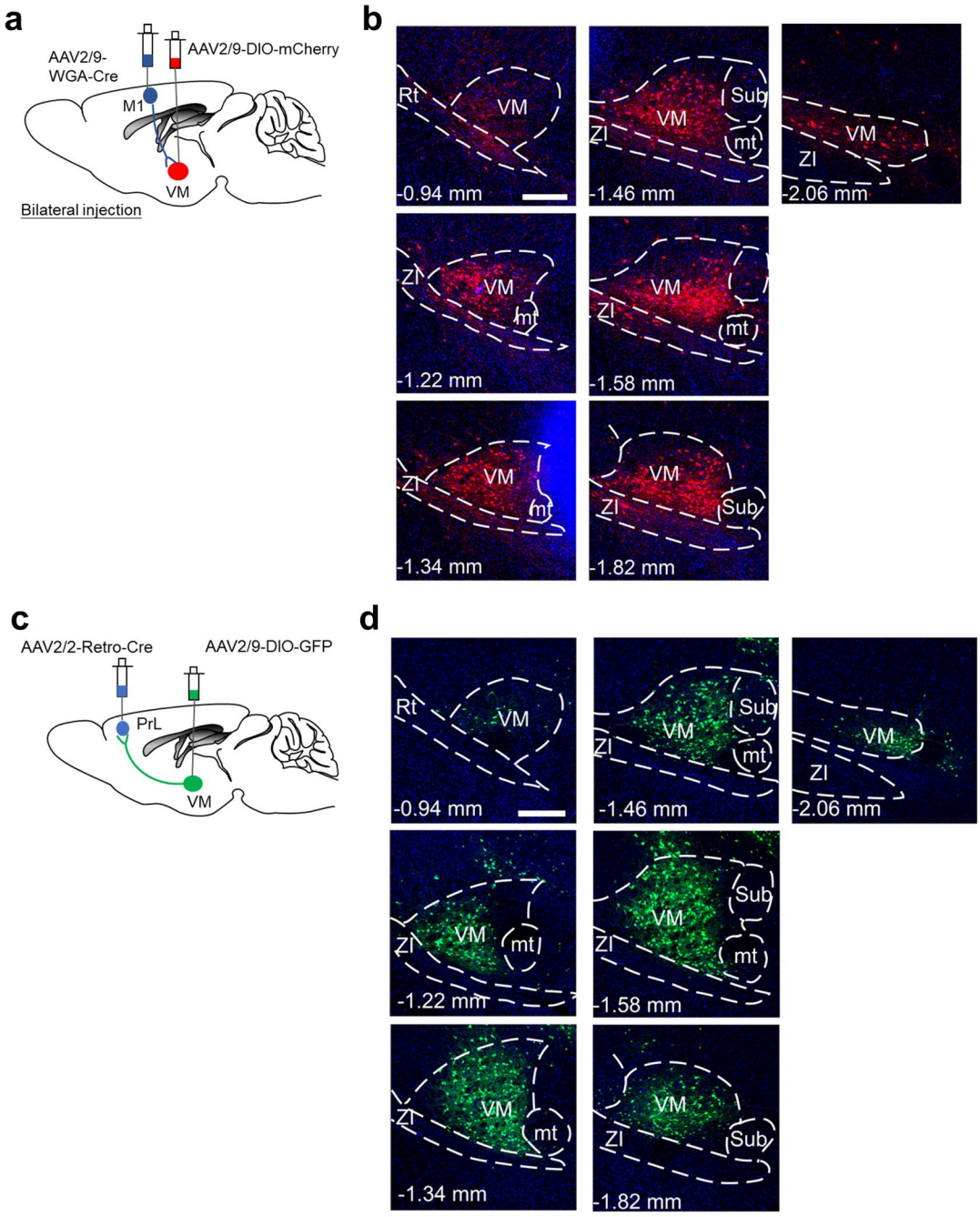

Figure S7. Spatial distribution of VM neurons from both antero- and retro-grade labelling. (a) Viral injection scheme of anterograde labelling from M1 region. **(b)** Fluorescent labelling of M1-innervaing VM neurons along the anteroposterior axis. Red, mCherry. Scale bar, 150 μm. **(c)** Viral injection scheme of regrograde labelling from PrL. **(d)** Fluorescent labelling of PrL-projecting VM neurons along the anteroposterior axis. Green, GFP. Scale bar, 150 μm.

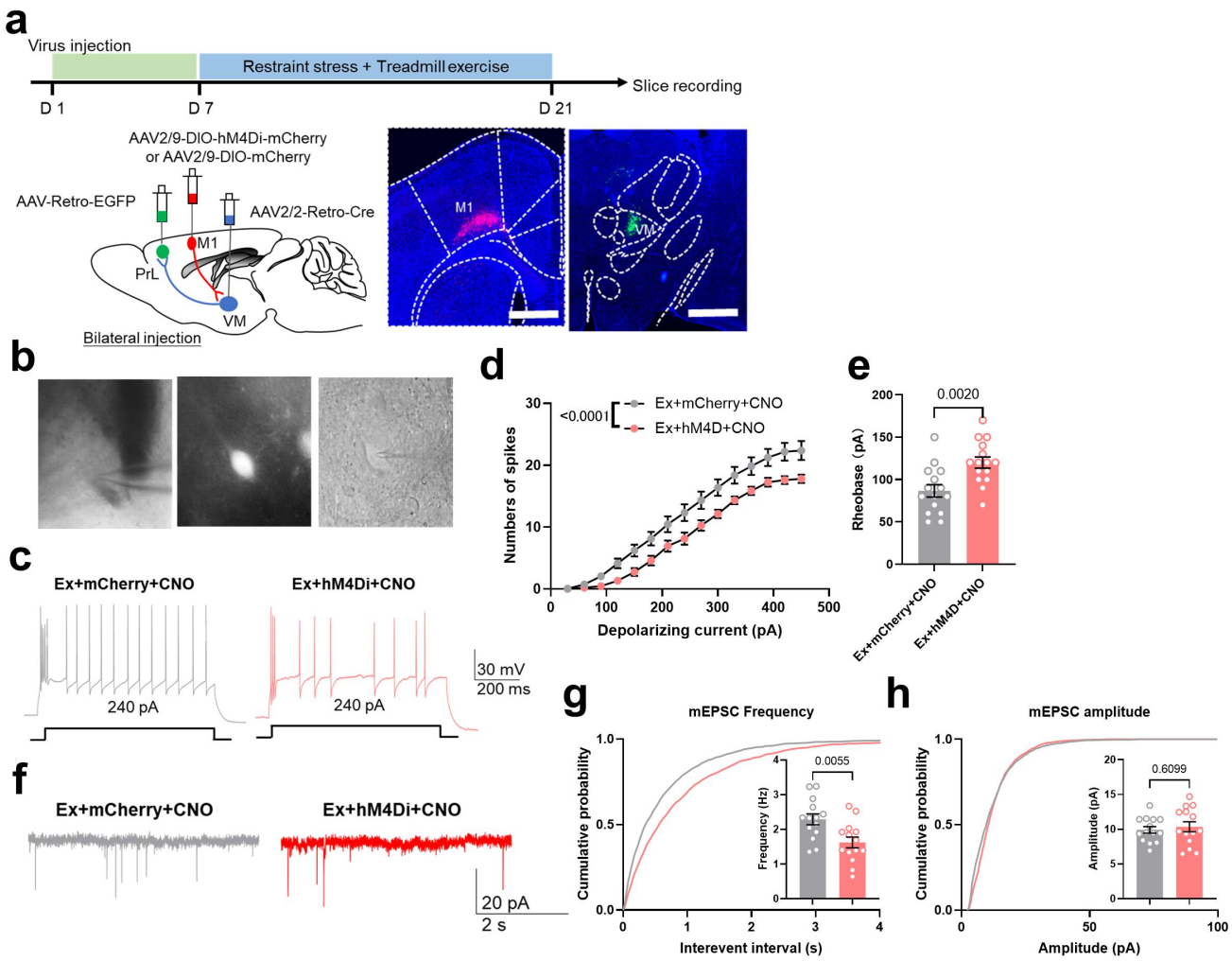

Figure S8. M1 input maintains the excitability of PrL-projecting VM nuclei. (a) Upper, timelines of experimental design. Lower left, viral injection sites. Lower right, distribution of PrL-projecting neurons in VM. Scale bar, 250 μm. **(b)** The patch-clamp recording of one representative cell. **(c)** Sample spikes of PrL-projecting VM neurons giving fixed (240 pA) injection currents. **(d)** Chemogenetic inhibition of M1 input depressed the total number of spikes in VM. Two-way ANOVA with respect to the group effect, $F(1,434)=89.46$, $P<0.0001$. **(e)** Inhibition of M1 inputs elevated rheobase of VM cells. Two-sample *t*-test, $t(28)=3.403$, $P=0.0020$. **(f)** Representative trances of miniature excitatory postsynaptic currents (mEPSCs) in all groups. **(g)** Distribution of mEPSC frequency. Inhibition of M1 inputs decreased the frequency of mEPSC. $t(28)=3.029$,

P=0.0055. **(h)** Distribution of mEPSC amplitude. Chemogenetic inhibition did not affect mEPSC amplitude. $t(28)=0.5165$, *P*=0.6099. *n*=15 neurons from 4 mice in each group. All data were presented as mean±sem.

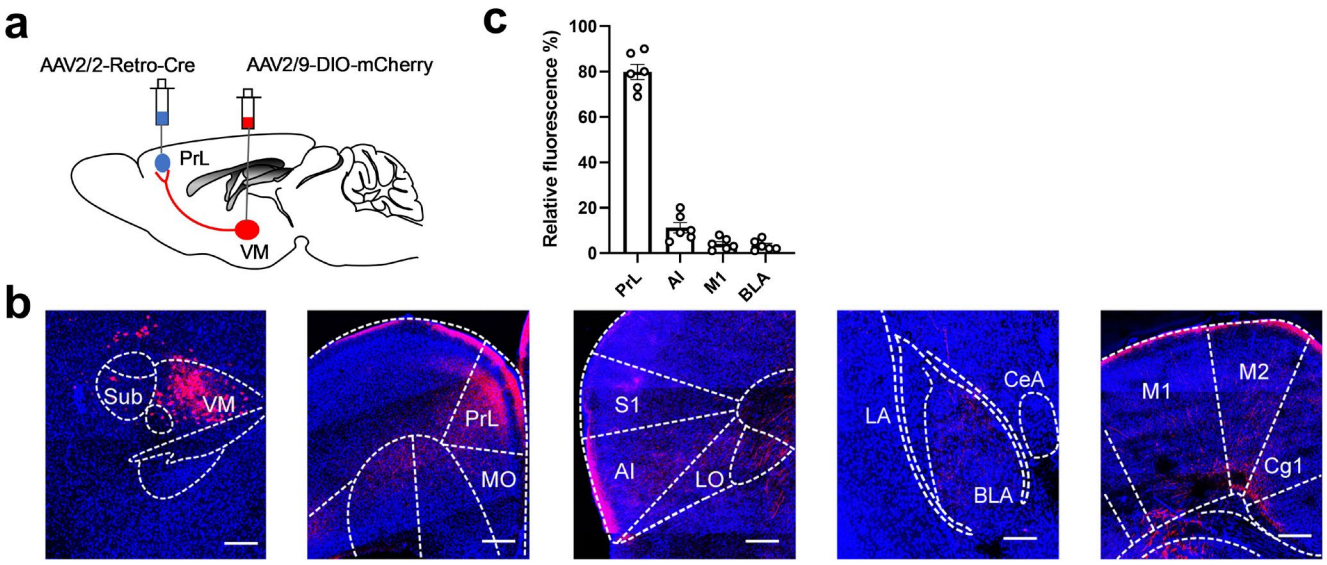

Figure S9. Spatial distribution of axonal terminals of PrL-projecting VM neurons. (a) Viral injection sites. **(b)** Representative fluorescent images showing the distribution of fibers of PrL-projecting VM neurons. Red, mCherry. Scale bar, 150 μm. **(c)** Relative fraction of axonal terminus (in fluorescent intensity) across brain regions. *N*=6 mice. All data were presented as mean±sem.